Acoustic emission response characteristics of anthracitic coal under uniaxial compression

Feng Du
China University of Mining and Technology - Beijing Campus
Kai Wang (kaiwang@cumtb.edu.cn)
China University of Mining and Technology - Beijing Campus
Guojun Zhang
China University of Mining and Technology - Beijing Campus
Gongda Wang
China Coal Technology and Engineering Group Corp
Qian Zhang
China University of Mining and Technology - Beijing Campus
Ji Ma
China University of Mining and Technology - Beijing Campus

Research

Keywords:

Posted Date: July 20th, 2020

DOI: https://doi.org/10.21203/rs.3.rs-42019/v1

Acoustic emission response characteristics of anthracitic coal under uniaxial compression

Feng Du[a,b], *Kai Wang*[a,b*], *Guojun Zhang*[c*], *Gongda Wang*[d], *Qian Zhang*[b], *Ji Ma*[a]

a Beijing Key Laboratory for Precise Mining of Intergrown Energy and Resources, China University of Mining and Technology (Beijing) 100083, China

b School of Emergency Management and Safety Engineering, China University of Mining & Technology (Beijing), Beijing 100083, China

c. State Key Laboratory of Groundwater Protection and Utilization by Coal Mining (China Energy Investment Corporation Ltd), Beijing 102209, China

d School of Civil and Resources Engineering, University of Science and Technology Beijing, Beijing 100083, China

E-mail：kaiwang@cumtb.edu.cn (K. Wang)

cherish-guojun@hotmail.com (G. Zhang)

Abstract: The damage evolution of coal is accompanied by the generation of acoustic emission (AE) signal. Through the analysis and research of AE response characteristics of coal deformation and failure, it is helpful to reveal the initiation, propagation and fracture evolution of micro cracks in coal. In this work, taking the anthracite coal as research object, the basic mechanical parameters of coal samples were obtained by ultrasonic tests and uniaxial compression experiments. Meanwhile, the AE response characteristics of coal samples during uniaxial compression were obtained through AE experiments. The results show that when the density is low, the wave velocity of coal sample decreases with the increase of density. When the density is higher than a certain value, the wave velocity of coal sample increases with the increase of density. Through the measurement of ultrasonic wave velocity, it is found that there are some non-uniformity and anisotropy in raw coal samples. The distribution of ring count, energy count and AE events with time in uniaxial compression process is approximately normal distribution. The AE events are concentrated in the elastic stage and yield stage, and the energy amplitude of AE events is higher in the plastic stage. Compared with the ring count and energy count, the AE events have good positioning function, which can better reflect the evolution of internal cracks in coal samples during uniaxial compression.

Key words: Anthracite coal; deformation failure; uniaxial compression; acoustic emission; space-time evolution

1 Introduction

With the coal resources gradually entering the deep mining, under the complex environment of "three high and one disturbance", the coal and rock are more likely to break and lose stability, leading to more dynamic disasters such as rockburst and coal and gas outburst (Cheng et al. 2017; Fan et al. 2019, 2020; Yuan, 2015, 2016; Xie et al. 2017; Liu et al. 2020; Zhao et al. 2018). Moreover, in recent years, the coal-gas compound dynamic disaster, which shows both the characteristics of coal gas outburst and rockburst, has attracted more and more attention. And it has become increasingly serious, which has become a major disaster affecting China's energy security (Du and Wang 2019; Wang and Du, 2020; Pan 2016). Coal medium is a complex heterogeneous material, and there are a lot of microstructures such as cracks and pores inside the coal (Liu and Zhu, 2016; Liu et al. 2020; Liu et al. 2018). When these microstructures are stressed, the deformation, stress concentration and failure will occur, and the stored strain energy will be released in the form of elastic waves, which is the AE phenomenon of the coal rock under stress (Carpinteri et al. 2013a, 2013b; Yuan and Shi 2018). The AE signal during the failure of the coal reflects the microscopic destruction of coal and is closely related to the evolution of coal damage. Through in-depth analysis of the AE signals during the coal damage, the deformation and fracture process of the internal microstructures of coal can be inversed, which is helpful to reveal the evolution law of coal damage and provide references for fully understanding of the mechanism, forecasting and early warning of coal gas outburst, rockburst and coal-gas compound dynamic disaster.

Many scholars at home and abroad have done a lot of basic research work on the characteristics of AE in the process of coal damage. Shkuratnik et al. (2004) studied the AE characteristics of coal rock under uniaxial loading through experiments. By locating the acoustic emission source of coal samples under uniaxial compressive

stress, Masahiro et al. (1988) pointed out that the AE sources are distributed as a strip along the crack. Vishal et al. (2015) studied the mechanical properties of coal based on AE method and investigated the influence of CO_2 and moisture treatment on the strength of coal. Kong et al. (2015; 2016; 2017) introduced the AE critical slowing down theory of coal. They presented that the AE numbers and energy will increase with the increase of gas pressure, while the correlation dimension of AE parameters show the tendency of decrement. Du et al. (2018) systematically researched the acoustic emission characteristics of coal-rock combined bodies. Jiang et al. (2017) studied the AE characteristics and energy dissipation of coal under tiered cyclic loading. They indicated that the change of AE of coal under tiered cyclic loading could essentially present the result of coal damage. Song et al. (2020) studied the loading direction dependent anisotropy of coal under uniaxial compression based on AE technology. They also investigated the relationship between cumulative absolute AE energy and anisotropic angle. From the previous research results, the research mainly focused on the evolution characteristics of AE parameters and identification of precursor information of conventional coal rock damage. In fact, the spatial location of AE is the most intuitive reflection of the evolution process of material damage, and there are relatively few studies on the space-time evolution law of AE. At present, a lot of early warning research on AE to coal and rock dynamic disaster is based on coal gas outburst and rockburst, few researches about AE focus on the early warning of coal-gas compound dynamic disaster. Moreover, the AE theory of coal rock is not complete. A large number of systematic experimental studies of AE are still needed to reveal the relationship between AE signals and coal rock damage, and to analyze the space-time evolution characteristics of AE during coal rock damage, which will provide theoretical guidance for monitoring and early warning of coal rock instability and destruction by acoustic emission.

Based on the analysis above, in this work, taking anthracite coal as the research object, the basic mechanical parameters of the raw coal samples were obtained

through ultrasonic testing experiments and uniaxial compression experiments. Meanwhile, the AE response characteristics of raw coal samples in uniaxial compression process were obtained by AE experiment, which provides theoretical guidance for AE monitoring and early warning of failure of coal and rock dynamic disasters.

2 Coal Samples and experimental system

2.1 Collection and preparation of coal samples

The anthracite coal samples used in the experiments were collected from the 3313 working face of 3# coal panel in Tang'an coal mine, Jincheng, Shanxi Province. After the coal is collected, it was wrapped immediately with fresh-keeping film to prevent the weathering of the coal. During the transportation of the coal, several layers of foam film were wrapped to prevent the colliding of the coal blocks and destroy the original joints and cracks to create new fissures. The selected large raw coal was first cut into a 102 mm×51 mm×51 mm cuboid using a rock cutting machine, and then the six sides of the coal samples were polished by a double-end grinder. Through polishing, the unevenness of the six sides of the coal samples is less than 0.01 mm. Finally, the standard coal samples used for uniaxial compression and AE test were obtained, as shown in Figure 1.

Fig. 1 Schematic diagram of coal samples

2.2 Ultrasound test

Ultrasonic test was performed on all standard cube samples, and several samples with the closest wave velocity were selected for mechanical experiments and AE

experiments to ensure that the conclusions drawn in this work are reasonable and reliable. The ZBL-U520 non-metallic ultrasonic detector were used for ultrasonic test, and its accuracy of sound time measurement is ±0.05 μs. Its range of sound time measurement is 0~600000 μs. The amplifier bandwidth is 10 KHz~250 KHz and the receiving sensitivity is less than 30 μs. First, the vernier caliper was used to measure the length, width and height of coal sample, and electronic scale was used to measure the mass of the sample. Then, the ZBL-U520 non-metallic ultrasonic detector was used to measure the wave velocity of ultrasonic through coal sample, and the average value was measured three times at each position. The detection position is shown in Fig. 2. Finally, the basic size, mass, volume, density and ultrasonic wave velocity of the coal samples can be obtained, as shown in Table 1.

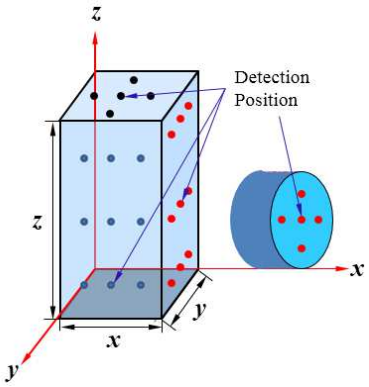

Fig. 2 Ultrasonic inspection position distribution of coal sample

Table 1 Preliminary parameters of coal samples

Number	Hight (z/mm)	Length (x/mm)	Wide (y/mm)	Quality (g)	Volume (cm^3)	Density (g/cm^3)	Wave velocity (km/s)			Mean	Variance
							z	x	y		
0	100.20	50.40	50.40	380.60	254.52	1.50	1.74	1.91	1.74	1.80	0.0096
1	100.00	50.00	50.00	441.80	250.00	1.77	2.54	3.25	2.68	2.82	0.1443
2	100.00	50.00	50.00	379.30	250.00	1.52	1.48	1.69	1.71	1.63	0.0166
3	100.00	50.00	50.00	444.70	250.00	1.78	2.54	2.81	2.65	2.67	0.0188
4	98.24	50.00	50.00	361.50	245.60	1.47	1.79	1.89	1.89	1.86	0.0034
5	98.30	50.02	50.06	354.40	246.14	1.44	1.97	1.73	1.80	1.83	0.0152
6	98.44	50.02	50.06	345.90	246.49	1.40	2.22	1.94	2.18	2.11	0.0229
7	72.40	45.90	45.90	228.20	152.53	1.50	1.60	1.63	1.78	1.67	0.0096
Mean						1.55	1.98	2.11	2.05	2.05	0.0039
Variance						0.02	0.17	0.35	0.16	0.23	0.0118

It can be seen from Table 1 that the density of the eight raw coal samples is 1.44 to 1.78 g/cm^3, with an average of 1.55 g/cm^3. The density of the sample varies greatly, and the variance of the density of the sample is 0.02. The main reason for the density difference of the raw coal samples is that in addition to the coal matrix, the raw coal sample also contains minerals such as quartz, calcite, and ankerite in different proportions. The ultrasonic wave velocity of the eight raw coal samples is 1.48~3.25 km/s, with an average of 2.05 km/s. The ultrasonic wave velocity changes greatly in the X direction, with a great variance of 0.35. The fluctuations in the Y and Z directions are relatively close, and the variances are 0.16 and 0.17 respectively, indicating that the distribution of joint fissures and minerals in the raw coal samples has obvious directionality. When the density of the raw coal sample is less than the average density of 1.55 g/cm^3, there is an approximately negative correlation between the density and the wave velocity. As the density of raw coal sample increases, the content of quartz and other minerals gradually increases. Quartz and other minerals are mainly dispersed in raw coal samples, resulting in more interlayer between coal and quartz, thus reducing the propagation speed of ultrasonic wave in raw coal samples. When the density is higher than the average density of 1.55 g/cm^3, there is an approximately positive correlation between the density and the wave velocity. As the density of raw coal sample continues to increase, the content of minerals such as quartz further increases. A relatively concentrated distribution area is formed in the raw coal sample to reduce the number of interlayer, thereby increasing the ultrasonic propagation speed in the raw coal sample, as shown Figure 3.

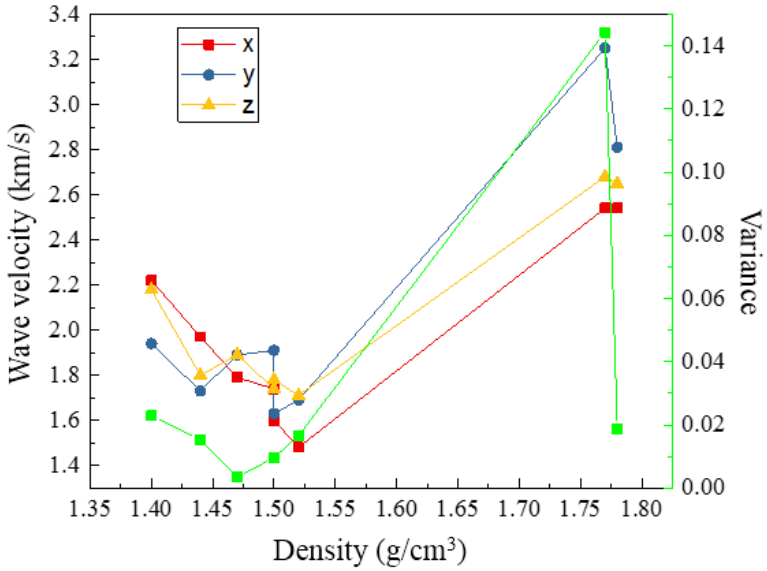

Fig. 3 Density and ultrasonic wave velocity of coal

For the same raw coal sample, there are still some differences in the wave velocity in the three directions, which also shows that there is a certain non-uniformity and anisotropy in the raw coal sample. The variance range of the ultrasonic wave velocity in the three directions is 0.0096~0.1443. Compared with different raw coal samples, the difference of ultrasonic wave velocity is small. Therefore, according to the result of ultrasonic wave velocity testing, we selects five raw coal samples whose wave velocities are relatively close, such as No. 0, 2, 4, 5, 6 for mechanical experiments and AE experiments.

2.3 Mechanical experiment and AE experiment system

The loading system used in the mechanical experiment is the WDW-100E microcomputer-controlled electronic multifunctional testing machine of the Beijing Computing Center. The system can perform uniaxial compression, brazilian splitting, drawing, bending, shearing and other experiments of coal rock. The maximum load is 100 kN, and the error is less than ± 0.5 %, which meets the basic requirements of the uniaxial compression test of the raw coal sample. The AE system is the PCI-2 system of the American Physical Acoustics Corporation (PAC). The system has a built-in 18-bit A/D converter, which is more suitable for low amplitude and low threshold (17 dB) settings. It has 4 high-pass and 6 low-pass filters. The frequency range of the

system is 1 kHz ~ 3 MHz, and the waveform sampling rate is as high as 10 m/s. There are eight optional parameter channels on PCI-2. Each channel has 16-bit A/D converter, and the speed is 10000/s. The system can realize parallel operation of multiple FPGA. In addition, the system can also be used as a digital signal processing card and provide Labview/C++ driver development program.

First, the BX120-3CA strain gauge was attached to the middle of the two adjacent sides of the raw coal sample. The grid size of the strain gauge is 3×2 mm, the resistance is $119.8_{\pm 0.3}\Omega$, and the sensitivity coefficient is $2.08_{\pm 1}\%$. Then, a multimeter was used to detect the resistance of the strain gauge. If the resistance range is between 119.5~120.1, the strain gauge is intact, otherwise the strain gauge should be replaced. The patching method of BX120-3CA strain gauge is shown in Figure 4.

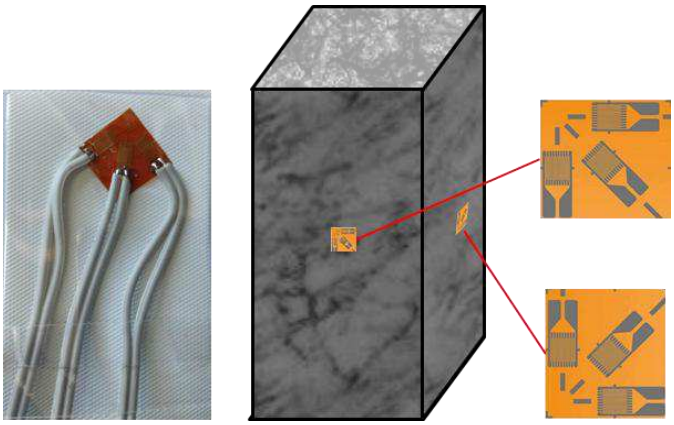

Fig. 4 BX120-3CA strain gauge and its patching method

After completing the above basic preparations, the noise was tested in the experimental environment. After testing, the threshold of the AE experimental system is fixed at 45 dB. The resonance frequency is 100 KHz~400 KHz. The sampling rate is 1 MSPS, and six sensors were used to collect and localize AE signals. Among them, the No. 1, 2 and 3 sensors are located at 10 mm from the upper edge of the raw coal sample, and the No. 4, 5 and 6 sensors are located at 10 mm from the lower edge of sample, as shown in Figure 5. The six AE sensor channel parameters and three-dimensional positioning settings are shown in Table 2.

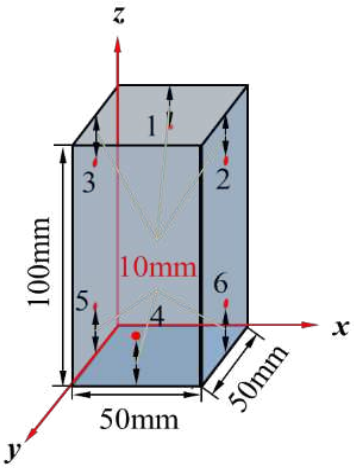

Fig. 5 AE sensor spatial distribution

Table 2 AE channel and positioning settings

Number	PDT/μs	HDT/μs	HLT/μs	Definition value/mm	Locking value/mm	Positioning length value/mm
1~4	50	150	200	78.0000	156.0000	7.8000
5~6	200	800	1000			

In order to make the probes of the six AE sensors fully contact with the raw coal sample, petroleum jelly was used as the coupling agent to fix the sensor on the surface of the raw coal sample to weaken the attenuation of the AE signal. Meanwhile, the water-proof tape was used for auxiliary fixing. The uniaxial compression loading system for raw coal sample and AE test system are shown in Figure 6.

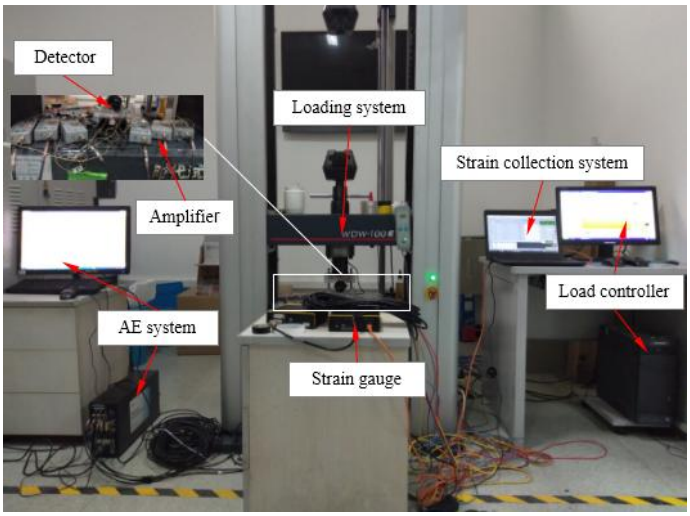

Fig.6 WDW-100E universal testing machine and AE system

3 Experimental results

3.1 Uniaxial compression test

The WDW-100E universal testing machine was used to carry out uniaxial compression test, and the basic mechanical parameters of raw coal samples were obtained, such as the whole stress-strain curve, compressive strength and Poisson's ratio. In the process of uniaxial compression, the loading speed is 0.2 mm/min, and the stress-strain value of coal sample is continuously recorded until the coal is damaged. Meanwhile, the stress of raw coal sample is obtained by the pressure sensor of universal testing machine, and the strain is obtained by the strain gauge connected with the strain gauge of raw coal sample.

Uniaxial compression tests were carried out on samples of No. 0, 2, 4, 5 and 6, and the stress-strain curve of raw coal samples was obtained, as shown in Fig. 7. The results show that the uniaxial compressive strength of five samples are 9.31 MPa, 6.32 MPa, 7.70 MPa, 13.92 MPa and 10.06 MPa respectively. The linear elastic modulus of five samples are 1.79 GPa, 1.29 GPa, 1.30 GPa, 2.00 GPa and 1.69 GPa respectively. The Poisson's ratio of five samples are 0.34, 0.31, 0.33, 0.30 and 0.35, respectively.

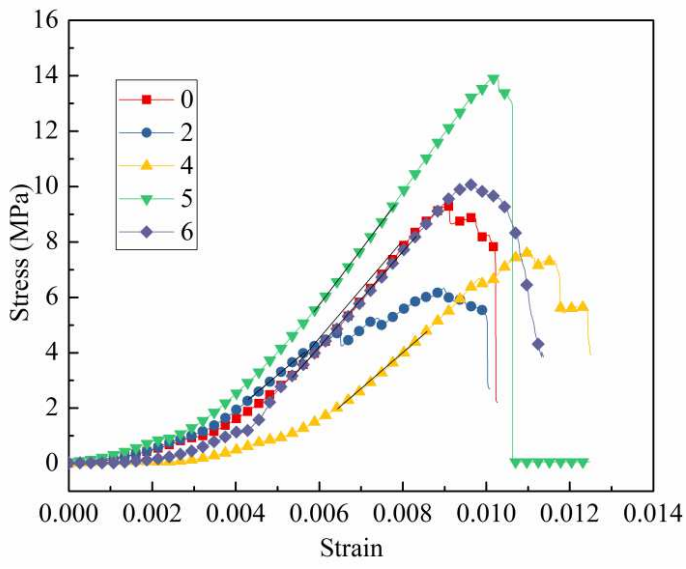

Fig. 7 Stress-strain relationship of coal samples under uniaxial compression

The bulk modulus and shear modulus of the coal can be expressed as,

$$\left.\begin{aligned} G &= \frac{E}{2(1+\mu)} \\ K &= \frac{E}{3(1-2\mu)} \end{aligned}\right\} \tag{1}$$

where G is the shear modulus and K is the bulk modulus. E is the young's modulus and μ is the Poisson's ratio.

According to equation (1), the relationship between bulk modulus, shear modulus and Poisson's ratio can be obtained as,

$$\mu = \frac{3K-2G}{6K+2G} \tag{2}$$

The Poisson's ratio distribution of coal is mainly in the range of 0-0.5. By further sorting out equation (2), the following formula can be obtained,

$$\eta = \frac{3(1-2\mu)}{2(1+\mu)} \tag{3}$$

where, η is the ratio of shear modulus G to bulk modulus K (η=g/k). μ is Poisson's ratio. Given that the Poisson's ratio range is 0-0.5, the value range of η is 0-1.5.

The Poisson's ratio of coal material is not only related to G and K, but also to internal friction angle. Sun (1988) deduced shear failure strength criterion of continuous medium rock mass based on Mohr-Coulomb strength criterion,

$$\mu = \frac{1}{2}(1-\sin\varphi) \tag{4}$$

In addition, Zhang (2011) study the Poisson's ratio and internal friction angle in-depth, and presented that there is $\mu \leqslant \tan\varphi(1-\sin\varphi)$ in brittle failure of rock. Therefore, it can be seen that the different of μ and φ directly affect the failure type of materials.

According to equations (1)-(4), the basic relationship between Poisson's ratio and internal friction angle can be obtained, as shown in Fig. 8.

If the yield process of the material satisfies the Mohr-Coulomb criterion, the relationship between the uniaxial compressive strength and the cohesion and friction angle of the material is

$$\sigma_u = \frac{2c\cos\varphi}{1-\sin\varphi} \tag{5}$$

where σ_u is the uniaxial compressive strength, MPa. c is the cohesion, MPa.

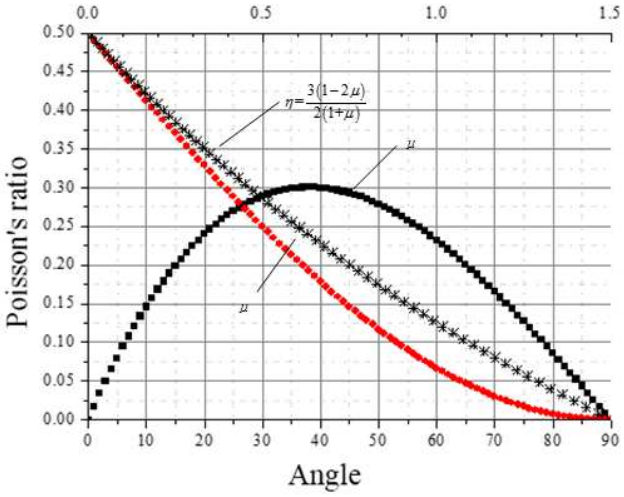

Fig. 8 Relationship between Poisson's ratio and friction angle

Finally, the basic mechanical parameters of five coal samples can be calculated by uniaxial compression test, as shown in Table 3.

Table 3 Mechanical parameters obtained from the experiment

Number	Compressive strength /MPa	Linear elastic modulus /GPa	Poisson's ratio	Internal friction angle/°	Bulk modulus /GPa	Shear modulus /GPa	Cohesion /MPa
0	9.31	1.79	0.34	18.65	1.86	0.67	3.42
2	6.32	1.29	0.31	21.80	1.16	0.49	2.27
4	7.70	1.30	0.33	20.12	1.26	0.49	2.61
5	13.92	2.00	0.30	23.66	1.66	0.77	4.86
6	10.06	1.69	0.35	17.39	1.88	0.63	3.29
Average	9.46	1.61	0.33	20.32	1.57	0.61	3.29

Note: Since Poisson's ratio of raw coal samples is greater than or equal to 0.3, the calculation of friction angle is based on formula (4).

It shows that although the selected raw coal samples are taken from the same block coal and the wave velocity is relatively consistent, the mechanical properties are still different, which further proves the heterogeneity of coal. The enlightenment to us is that in order to reduce the experimental error and wrong conclusion, it is necessary to select more coal samples for repeated experiments on the basis of economy and convenience.

3.2 AE response characteristics

The AE test and uniaxial compression test are carried out at the same time. Due to the failure of the AE instrument, we have not collected all the AE signals in the process of uniaxial compression test. Only the AE response signals of No. 0, 2, 4 and 5 raw coal samples were collected. Therefore, the AE response characteristics of No. 0, 2, 4 and 5 raw coal samples were only analyzed in this paper.

3.2.1 Ring count analysis of AE signal

The ring count of AE signal refers to the number of times that the AE signal exceeds the set threshold, which can roughly reflect the intensity and frequency of the signal. The relationship between AE ring count, axial stress and time is shown in Fig. 9.

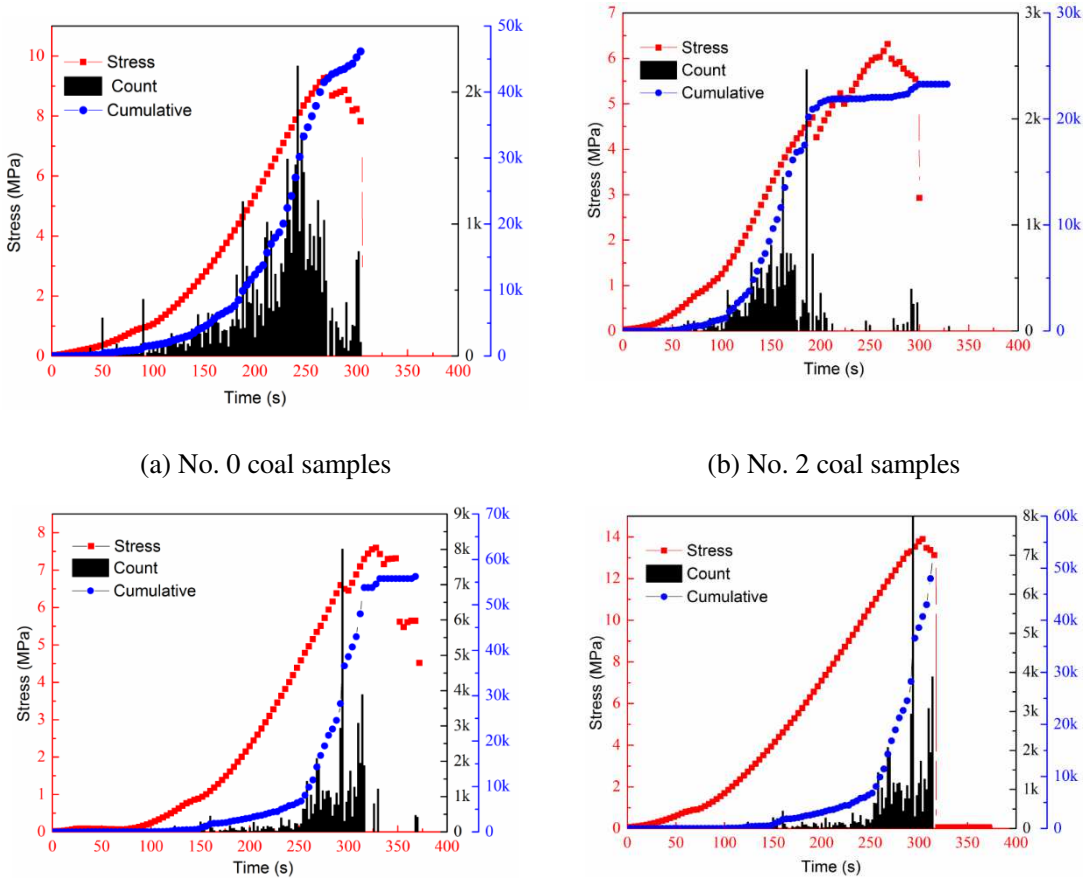

(a) No. 0 coal samples

(b) No. 2 coal samples

(c) No. 4 coal samples

(d) No. 5 coal samples

Fig. 9 Relationship between AE ring count, stress and time

It can be seen from Fig. 9 that the distribution of ring count with time in uniaxial

compression process is approximately normal distribution. The AE ring count is mainly concentrated in the linear elastic stage and plastic deformation stage of raw coal sample, and the maximum value of ring count appears in the plastic deformation stage of raw coal sample. The change of cumulative ring count value is in line with the change law of axial stress of raw coal sample during uniaxial compression. According to the complete stress-strain zoning of coal, the stress-strain relationship is related to the compaction, formation, development and expansion of internal cracks, and the corresponding pulse elastic wave is formed during the compaction, formation, development and expansion of cracks. By analyzing the change characteristics of ring count, the formation, development and expansion characteristics of internal cracks in raw coal samples can be obtained.

3.2.2 Energy characteristic analysis of AE signal

The energy of AE signal is the reflection of relative energy or relative intensity in AE events, and is less affected by threshold, operating frequency and propagation characteristics. The relationship between AE energy count and axial stress and time of raw coal sample during uniaxial compression is shown in Fig. 10.

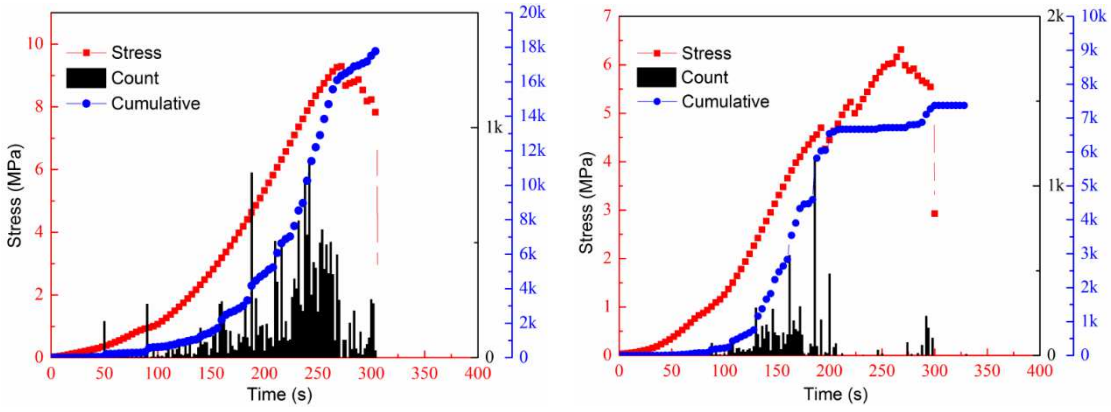

(a) No. 0 coal samples

(b) No. 2 coal samples

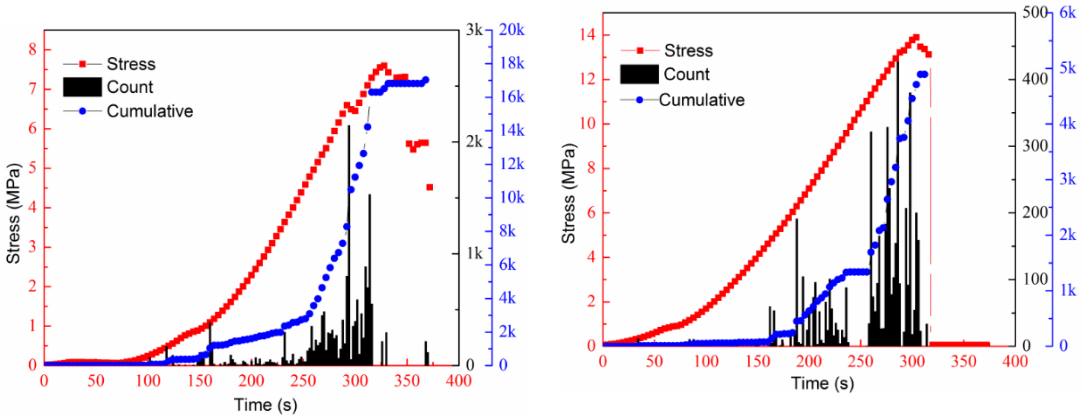

(c) No. 4 coal samples (d) No. 5 coal samples

Fig. 10 Relationship between AE energy, stress and time

It can be seen from Fig. 10 that the distribution of energy count with time during uniaxial compression is approximate to normal distribution. The AE energy count mainly concentrates in the linear elastic stage and plastic deformation stage of raw coal sample, and the maximum value of ring count appears in the plastic deformation stage of raw coal sample. The energy count and its cumulative value are close to the axial stress change in the uniaxial compression process. Therefore, the energy and ring count both can reflect the formation, development and expansion of the cracks in the raw coal sample during uniaxial compression.

3.3.3 Event analysis of AE signal

The AE events refer to the local changes in the interior of materials, which can reflect the total amount and frequency of AE. They are usually composed of one or more impact events, which are mainly used to evaluate the activity and concentration of AE sources. The relationship between AE events and axial stress and time of raw coal sample during uniaxial compression is shown in Fig. 11.

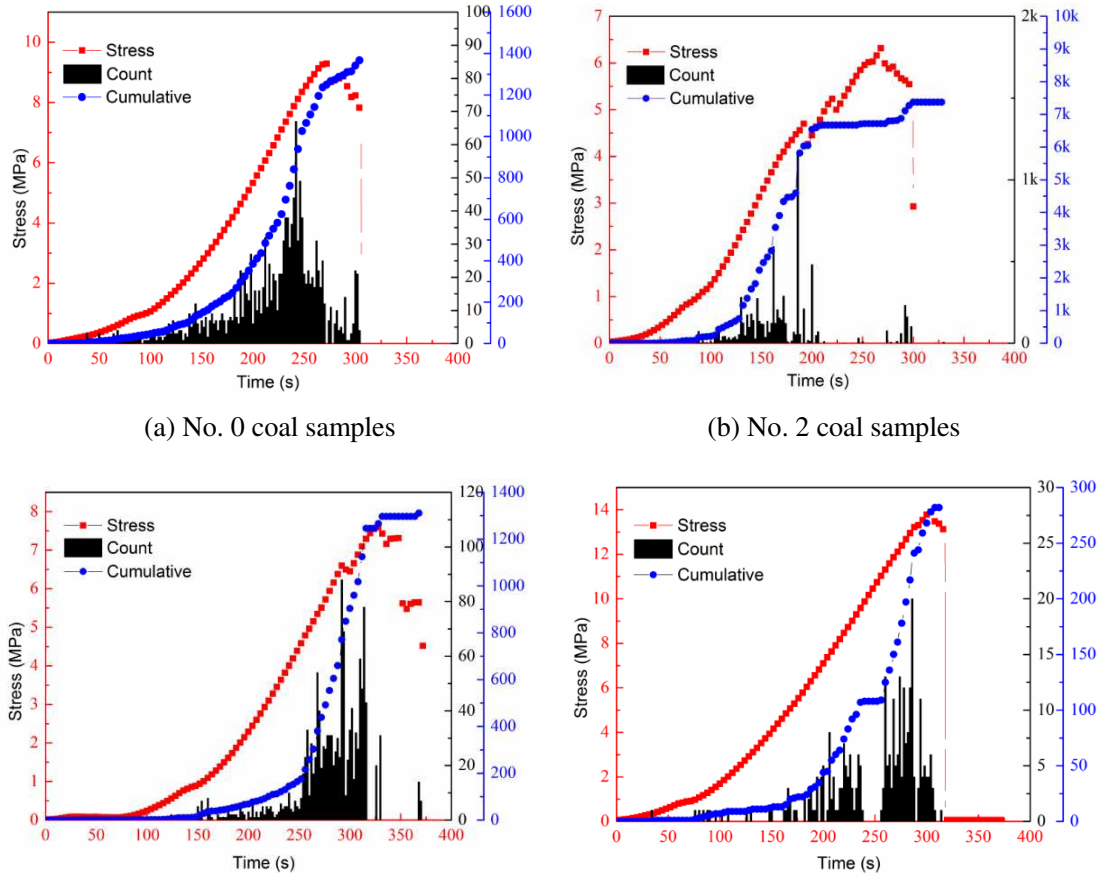

(a) No. 0 coal samples (b) No. 2 coal samples

(c) No. 4 coal samples (d) No. 5 coal samples

Fig. 11 Relationship between AE event, stress and time

It can be seen from Fig. 11 that the distribution of AE events with time during uniaxial compression is still approximate to normal distribution. The AE events are mainly concentrated in the linear elastic stage and plastic deformation stage of raw coal samples, and the maximum value of AE events occurs in the plastic deformation stage of raw coal samples. The change of cumulative AE events is also close to the stress variation law of raw coal samples during uniaxial compression. The AE events and their cumulative value are still close to the ring count and their cumulative value. Compared with the ring count and energy count, AE events can better reflect the formation, development and expansion of cracks in the raw coal sample during uniaxial compression.

In order to more intuitively show the evolution law of AE events with time and space under uniaxial loading of raw coal samples and taking the axial stress of raw

coal samples in the loading process of 60%, 95%, 100% of the maximum compressive strength as nodes, the stress state of raw coal samples is divided into four stages. They are elastic stage (0 ~ 60%), yield stage (60% ~ 95%), plastic stage (95% ~ 100%) and post peak stage respectively. The AE events and their amplitude characteristics in different stages are statistically analyzed, as shown in Fig. 12.

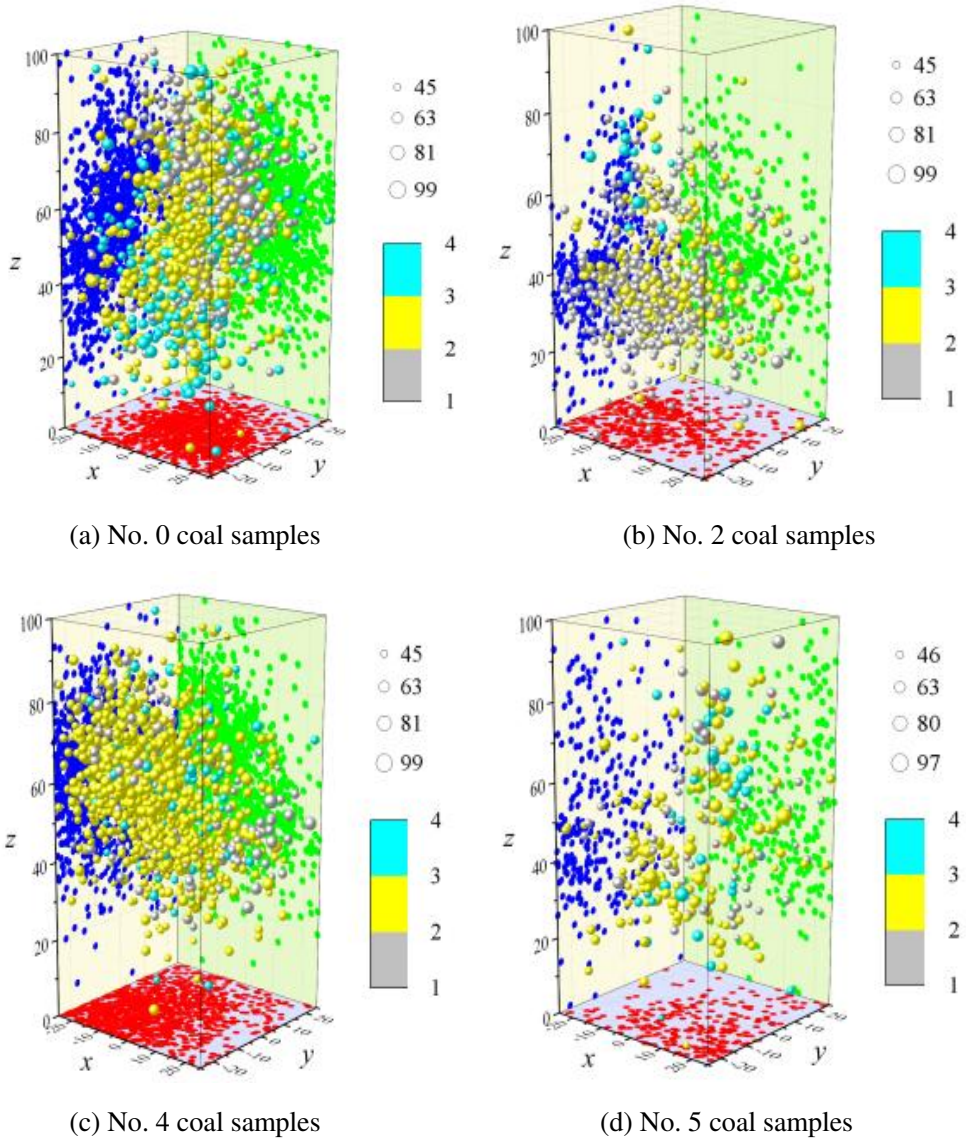

(a) No. 0 coal samples

(b) No. 2 coal samples

(c) No. 4 coal samples

(d) No. 5 coal samples

Fig. 12 AE source three-dimensional positioning

The numbers 1, 2, 3 and 4 on the color bars in Fig. 12 represent the elastic stage (0 ~ 60%), yield stage (60%~ 95%), plastic stage (95% ~ 100%) and post peak stage, respectively. Four spheres with different diameters represent the energy amplitudes of different AE events. According to the final statistics, the number of AE events in the

elastic stage of the four raw coal samples are 401, 324, 120 and 64, and the average energy amplitudes are 69.28, 63.58, 64.82 and 66.52 respectively. The AE events in the yield stage are 705, 166, 1046 and 177, and the average energy amplitudes are 54.43, 63.84, 64.45 and 66.51 respectively. The AE events in the plastic stage are 136, 1, 63 and 31, with an average of 69.28, 63.58, 64.82 and 66.52 respectively. The energy amplitudes were 69.54, 86, 64.21 and 69.94, respectively. The number of AE events in post peak stage was 125, 16, 39 and 11, and the average energy amplitude was 67.68, 72.13, 64.64 and 73.10, respectively. It can be seen from Fig. 12 that the AE events are mainly concentrated in the elastic stage and yield stage. At this stage, the original fracture experienced the process of compaction and then opening. However, in the plastic stage, the number of AE events is small, while the energy amplitude is large. This is due to the formation of new fractures and the increase of AE event energy amplitude. It is concluded that the AE events have a good positioning function, which can accurately locate the specific location of AE events, and better reflect the evolution law of internal cracks in raw coal samples during uniaxial compression.

4 Discussion

The existing research results show that the occurrence of coal gas outburst and rockburst has a high degree of suddenness (Fan et al. 2020; Konicek et al. 2013; Lama and Bodziony 1998; María et al. 2007). Therefore, it not the fact that the coal gas outburst and rockburst could not be predicted and prevented. In fact, most of the coal gas outbursts and rockburst accidents present certain precursory characteristics before they occur, such as the sound of coal cannon, spalling, coal body displacement. Predecessors have done a lot of research in this field. Similarly, the occurrence of coal-gas compound dynamic disaster is also induced by the instability of coal and rock. As for coal-gas compound dynamic disaster, before the failure of coal and rock, it will still release and produce a large number of AE signals, which has important practical significance for the study of AE evolution law in the process of coal and

rock damage. In this work, we obtained the AE response characteristics of anthracitic coal under uniaxial compression and focused on the similarities and differences of the ring count, energy count and AE events with time in uniaxial compression process. The distribution of all these three AE parameters with time during uniaxial compression is approximate to normal distribution and they all could slightly reflect the evolution process of cracks in coal rock fracture process. However, through the location study of AE events, it is found that AE events have a good positioning function, which can accurately locate the specific location of AE events, and better reflect the evolution law of internal cracks in raw coal samples during uniaxial compression. Therefore, in the engineering practice of the prevention of coal-gas compound dynamic disaster, the AE events can be used as one of the main AE characteristic parameters. The results of spatial location of AE events in front of the working face could be used to predict the fracture and instability of coal and rock, which is also conducive to the prediction of coal-gas compound dynamic disaster and improve the accuracy of its prediction. The preliminary study of this work is supposed to suggest researcher to study in-depth the mechanism of coal-gas compound dynamic disaster using AE technology.

The research in this work also shows that although the selected raw coal samples are taken from the same block coal, the mechanical properties are still different. As a result, the AE signal may jump and have large dispersion. The enlightenment to us is that the prediction of coal-gas compound dynamic disaster by using AE characteristics of coal should also be based on long-term monitoring. In this work, the characteristics of acoustic emission of coal and rock in the process of coal-gas compound dynamic disaster are only carried out in the laboratory scale, and the field scale test has not been designed. In the future, more in-depth research on the mechanism of coal-gas compound dynamic disaster based on AE technology is needed. Moreover, the continuous scale field monitoring of AE signal in the process of coal-gas compound dynamic disaster is the focus of our future research.

5 Conclusion

(1) For the same raw coal sample, there are some differences in the wave velocities in three directions, which indicates that the raw coal sample has certain non-uniformity and anisotropy.

(2) The distribution of ring count, energy count and AE events with time in uniaxial compression process is approximate to normal distribution, and these three parameters are close to the variation law of axial stress of coal during uniaxial compression. Through the change characteristics of these three parameters, the formation, development and expansion characteristics of internal cracks in raw coal samples can be obtained.

(3) AE events are concentrated in the elastic stage and yield stage, and the energy amplitude of AE events is higher in the plastic stage. Compared with ring count and energy count, AE events have a good positioning function, which can better reflect the evolution of internal cracks in raw coal samples during uniaxial compression.

Acknowledgments

This research is financially supported by the National Natural Science Foundation of China (51874314), the State Key Research Development Program of China (2018YFC0604501), the Chinese Postdoctoral Science Foundation (2019M660861).

Conflicts of Interest: All the authors declare that they have no conflict of interest.

Contributions

FD: Methodology; Writing-Original Draft. KW: Supervision; Writing-Review & Editing. GZ: Writing-Review & Editing. GW: Data processing. QZ: Experiments. JM: Experiments.

References：

Carpinteri A, et al. (2013a) Influence of damage in the acoustic emission parameters. Cement and Concrete Composites 44 (44): 9-16.

Carpinteri A, Corrado, M, Lacidogna, G, (2013b) Heterogeneous materials in compression: correlations between absorbed, released and acoustic emission energies. Engineering Failure Analysis 33 (7): 236-250.

Cheng Y, Jiang H, Zhang X, Cui J, Song C, Li X (2017) Effects of coal rank on physicochemical properties of coal and on methane adsorption. International Journal of Coal Science & Technology, 4(2):129-146.

Du F, et al. (2018) Investigation of the acoustic emission characteristics during deformation and failure of gas-bearing coal-rock combined bodies. Journal of Loss Prevention in the Process Industries 55: 253-266.

Du F, Wang K (2019) Unstable failure of gas-bearing coal-rock combination bodies: Insightsfrom physical experiments and numerical simulations. Process Safety and Environmental Protection 129: 264-279.

Fan C, Luo M, Li S, et al. (2019) A thermo-hydro-mechanical-chemical coupling model and its application in acid fracturing enhanced coalbed methane recovery simulation. Energies, 12, 626.

Fan C, Li S, Elsworth D, Han J, Yang Z (2020) Experimental investigation on dynamic strength and energy dissipation characteristics of gas outburst prone coal. Energy Science & Engineering 8 (4): 1015-1028.

Jiang C, et al. (2017) Experimental study on seepage properties, ae characteristics and energy dissipation of coal under tiered cyclic loading. Engineering Geology, 221: 114-123.

Kong X, et al. (2015) Critical slowing down on acoustic emission characteristics of coal containing methane. Journal of Natural Gas Science & Engineering 24: 156-165.

Kong X, et al. (2016) Fractal characteristics and acoustic emission of coal containing

methane in triaxial compression failure. Journal of Applied Geophysics 124: 139-147.

Kong X, et al. (2017) Time-varying multifractal of acoustic emission about coal samples subjected to uniaxial compression. Chaos, solitons & fractals 103: 571-577.

Konicek P, Soucek K, Stas L, et al. (2013) Long-hole destress blasting for rock-burst control during deep underground coal mining. International Journal of Rock Mechanics and Mining Sciences 61 (2013): 141-153.

Lama R, Bodziony J (1998) Management of outburst in underground coal mines. International Journal of Coal Geology 35 (1-4): 83-115.

Liu A, Wang K, Zang J, Du F, Zhou A (2018) Relative permeability of gas for unconventional reservoirs. Transport in Porous Media 124: 289-307.

Liu A, Liu S, Hou X, Liu P (2020) Transient gas diffusivity evaluation and modeling for methane and helium in coal. International Journal of Heat and Mass Transfer 159:120091.

Liu A, Liu S, Wang G, Sang G (2020) Modeling of coal matrix apparent strains for sorbing gases using a transversely isotropic approach. Rock Mechanics and Rock Engineering. doi:10.1007/s00603-020-02159-3.

Liu Y, Zhu Y (2016) Comparison of pore characteristics in the coal and shale reservoirs of Taiyuan Formation, Qinshui Basin, China. International Journal of Coal Science & Technology 3(3): 330-338.

María B, Díaz Aguado C, Nicieza González (2007) Control and prevention of gasoutbursts in coal mines, Riosa–Olloniego coalfield, Spain. International Journal of Coal Geology 69 (4): 253-266.

Masahiro Seto, Hidekazu Sato, Masaru Sato, Makoto Kohno (1988) Hypocenter distributions of ae in coal under uniaxial compression 104(1201): 163-168.

Pan Y (2016) Integrated study on compound dynamic disaster of coal-gas outburstand rockburst. Journal of China Coal Society, 41: 105-112.

Song H, Zhao Y, Derek E, Jiang Y, Wang J (2020) Anisotropy of acoustic emission in coal under the uniaxial loading condition. Chaos, Solitons & Fractals, (130): 109465.

Shkuratnik VL, Filimonov YL, Kuchurin SV (2004) Experimental investigations into acoustic emission in coal samples under uniaxial loading. Journal of Mining science, 40(5):458-464.

Sun GZ (1998) Structural mechanics of rock mass. Science Press, Beijing.

Vishal V, Ranjith P, Singh T (2015) An experimental investigation on behaviour of coal under fluid saturation, using acoustic emission. Journal of Natural Gas Science & Engineering 22: 428-436.

Wang K, Du F (2020) Coal-gas compound dynamic disasters in China: A review. Process Safety and Environmental Protection 133: 1-17.

Xie H, Ju Y, Gao F, Gao M, Zhang R (2017) Groundbreaking theoretical and technical conceptualization of fluidized mining of deep underground solid mineral resources. Tunnelling and Underground Space Technology 67: 68-70.

Yuan L (2015) Theory and practice of integrated coal production and gas extraction. International Journal of Coal Science & Technology 2(1): 3-11.

Yuan L (2016) Control of coal and gas outbursts in Huainan mines in China: a review. Journal of Rock Mechanics and Geotechnical Engineering 8 (4): 559-567.

Yuan R, Shi B (2018) Acoustic emission activity in directly tensile test on marble specimens and its tensile damage constitutive model. International Journal of Coal Science & Technology 5(3): 295-304.

Zhang X, et al. (2011) Study of relationship between Poisson's ratio and angle of internal friction for rocks. Chinese Journal of Rock Mechanics and Engineering 30(S1): 2599-2609.

Zhao B, Wen G, Sun H, Sun D, Yang H, Cao J, Dai L, Wang B (2018) Similarity criteria and coal-like material in coal and gas outburst physical simulation. International Journal of Coal Science & Technology, 5(2): 167-178.

Figures

Figure 1

Schematic diagram of coal samples

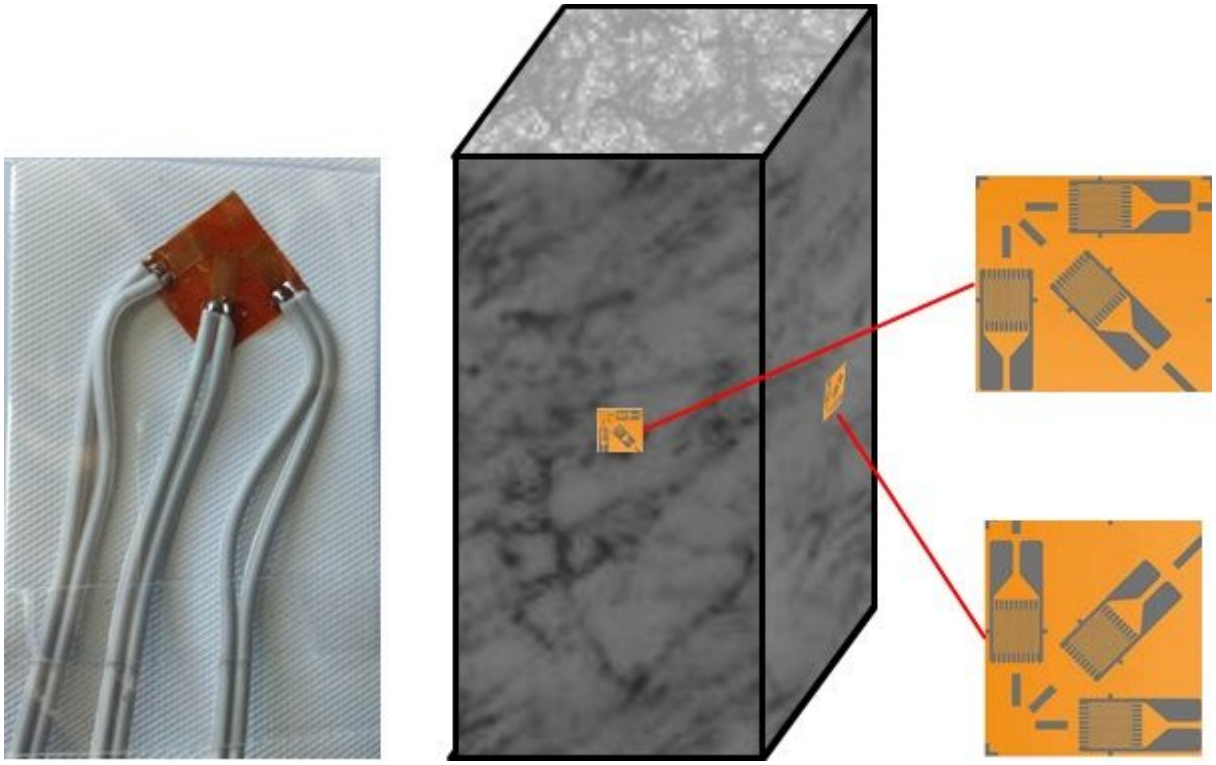

Figure 2

Ultrasonic inspection position distribution of coal sample Table 1 Preliminary parameters of coal samples

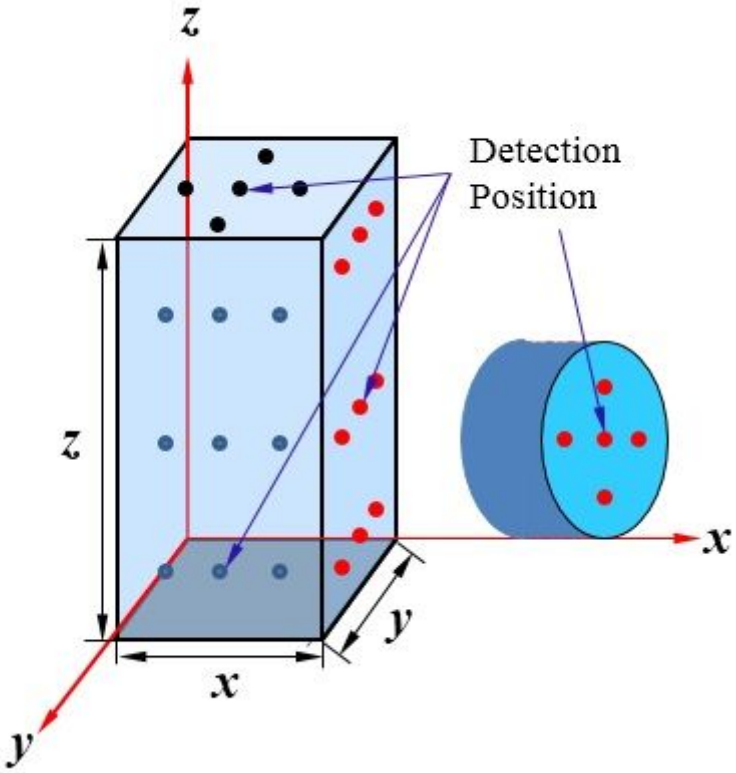

Figure 3

Density and ultrasonic wave velocity of coal

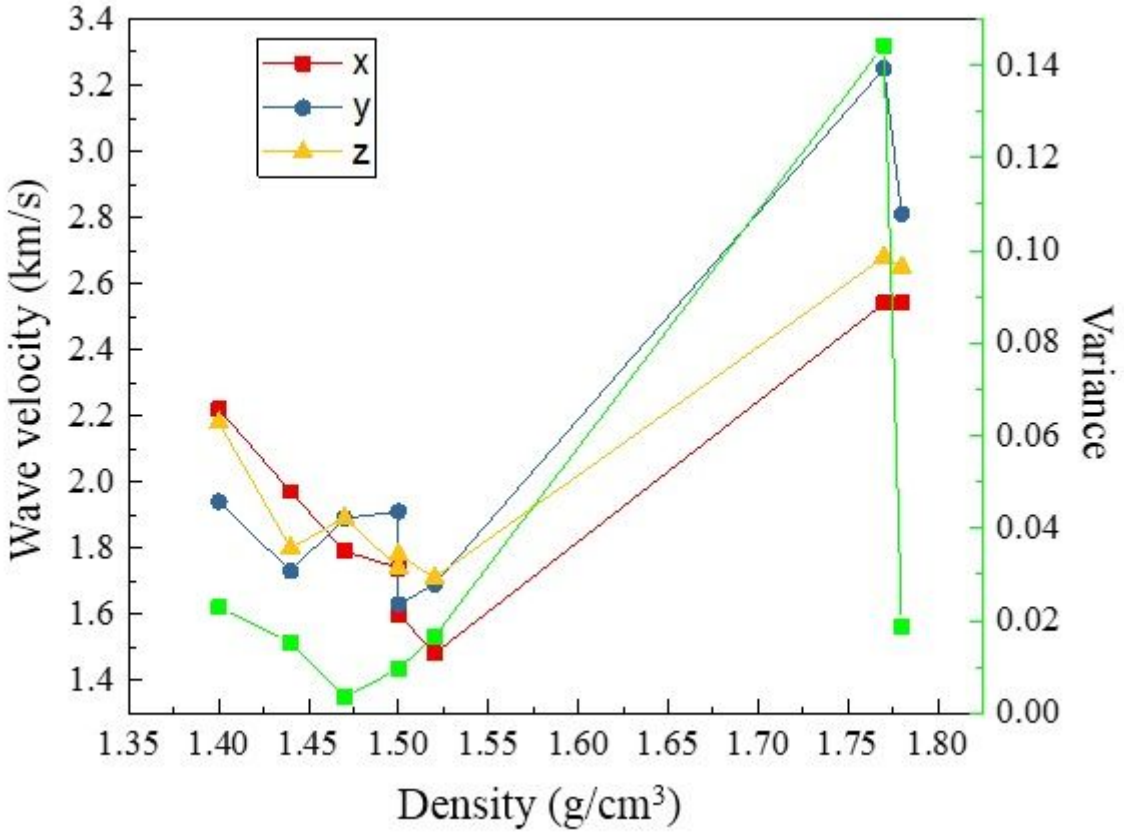

Figure 4

BX120-3CA strain gauge and its patching method

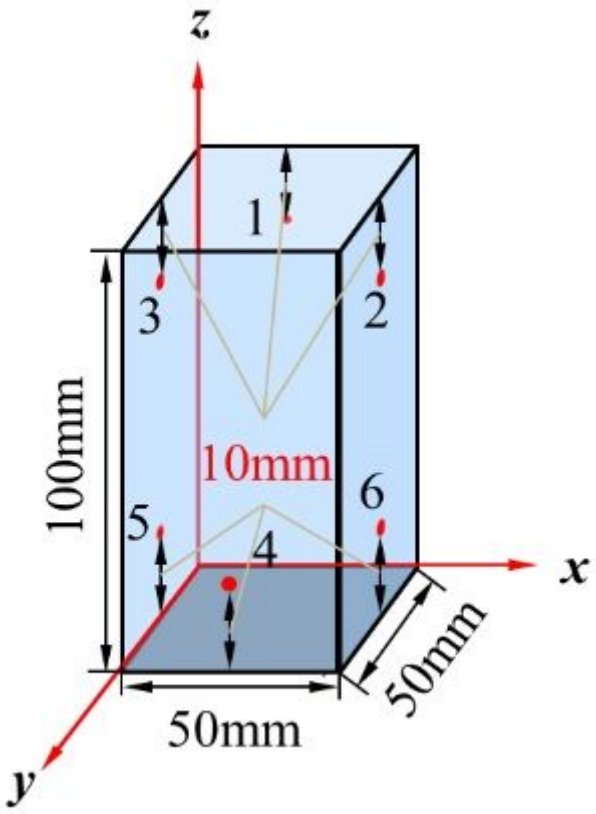

Figure 5

AE sensor spatial distribution

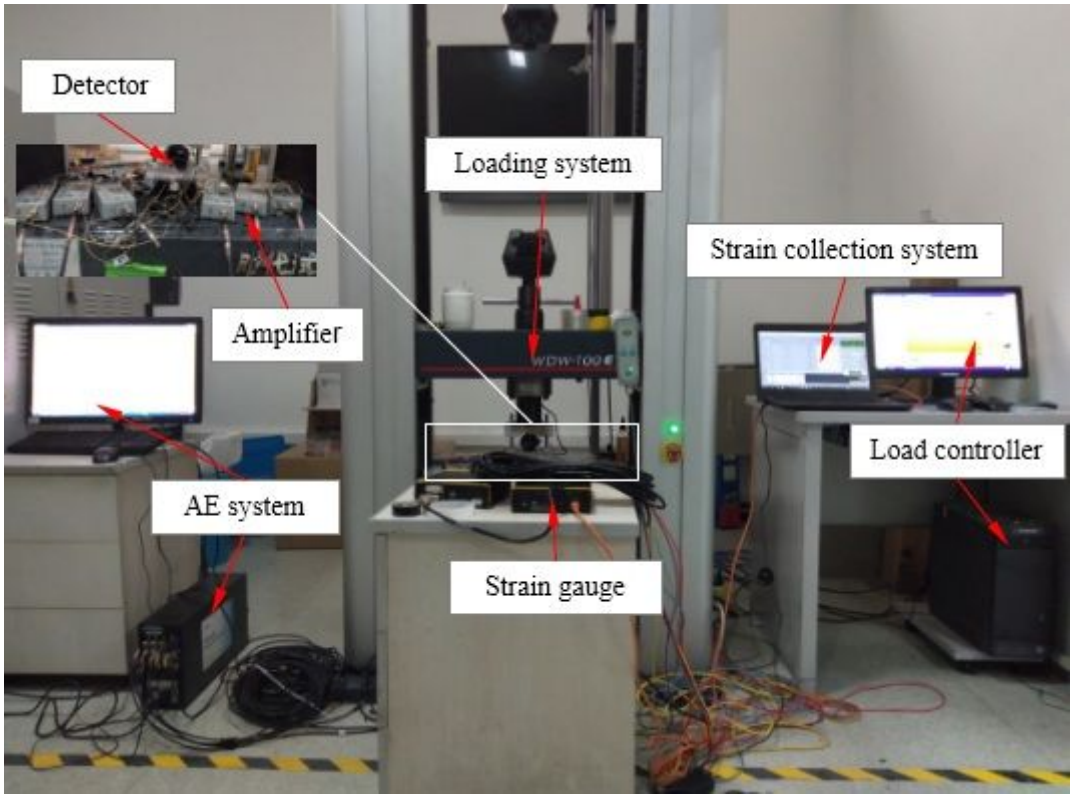

Figure 6

WDW-100E universal testing machine and AE system

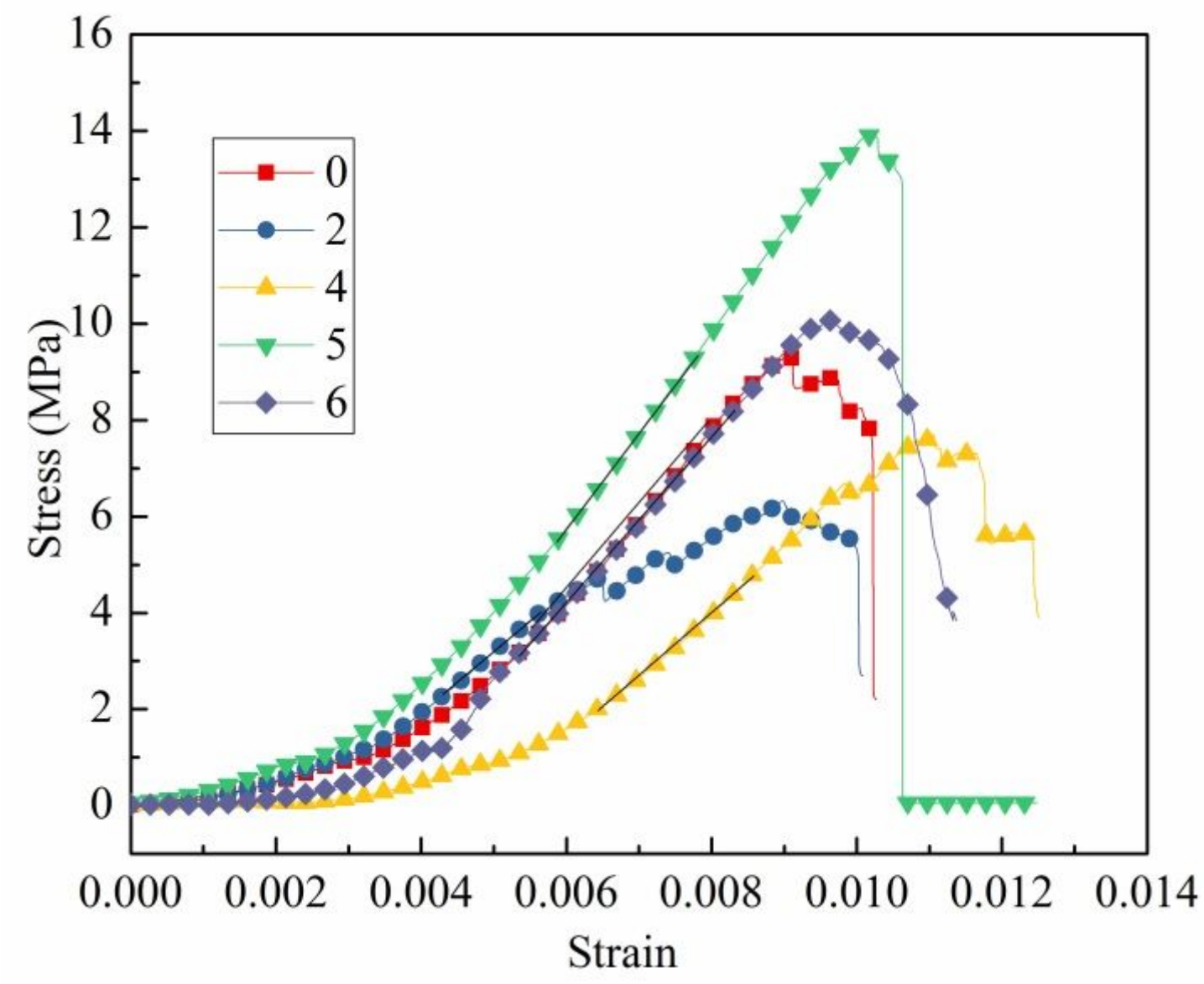

Figure 7

Stress-strain relationship of coal samples under uniaxial compression

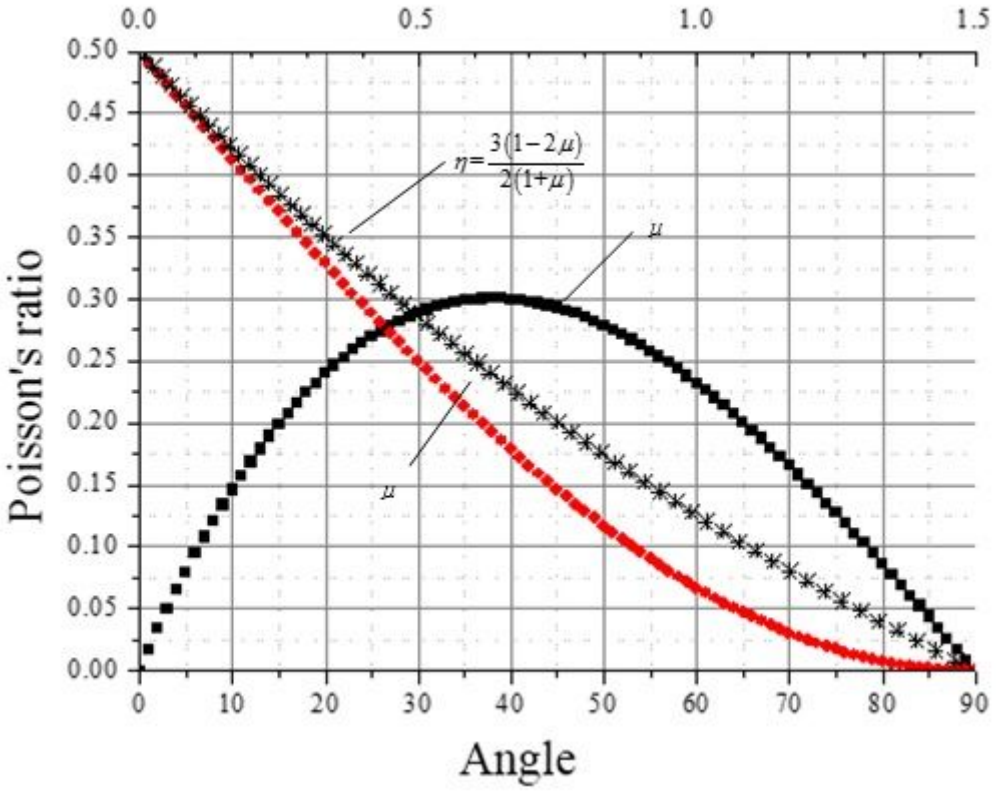

Figure 8

Relationship between Poisson's ratio and friction angle

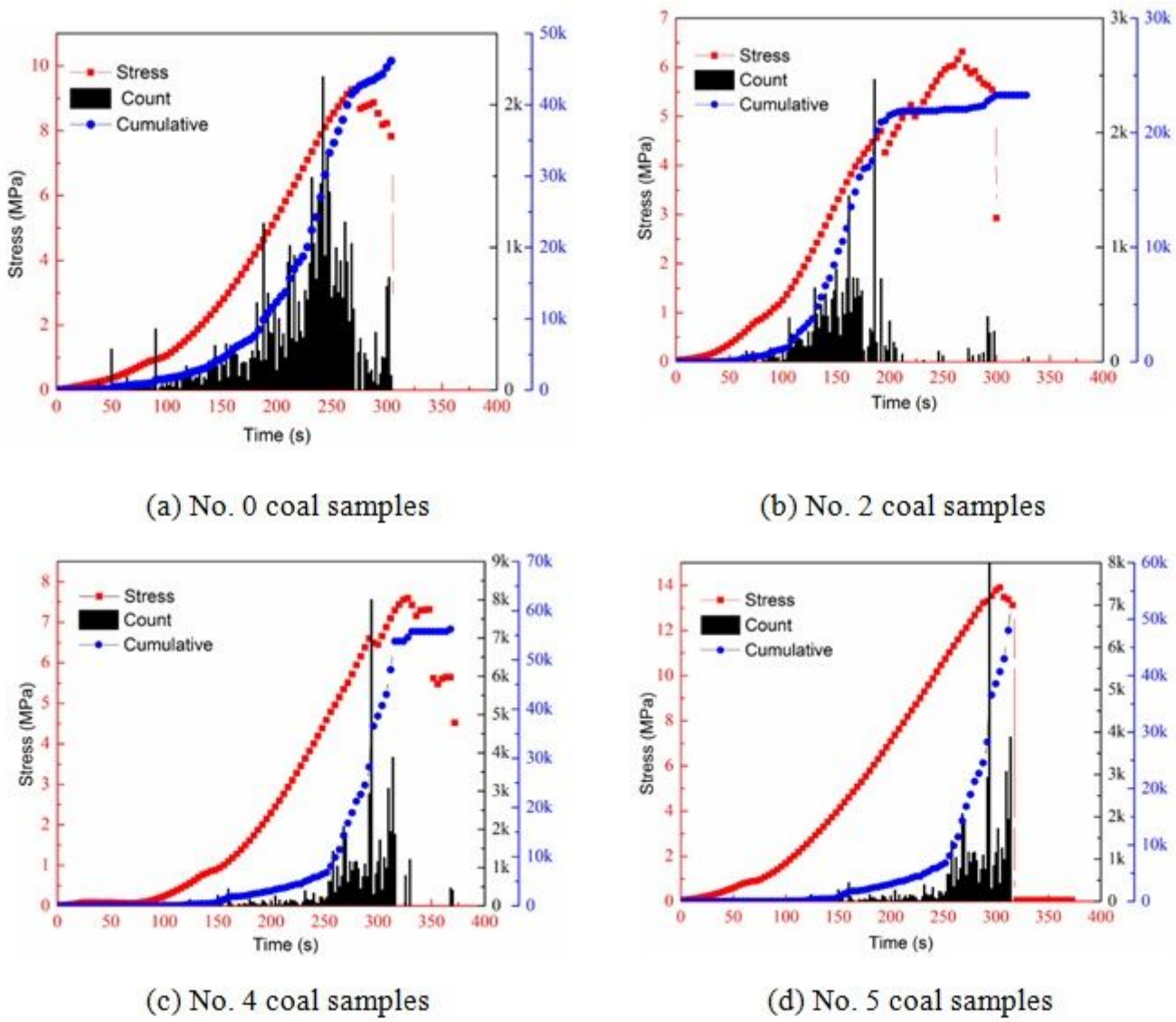

Figure 9

Relationship between AE ring count, stress and time

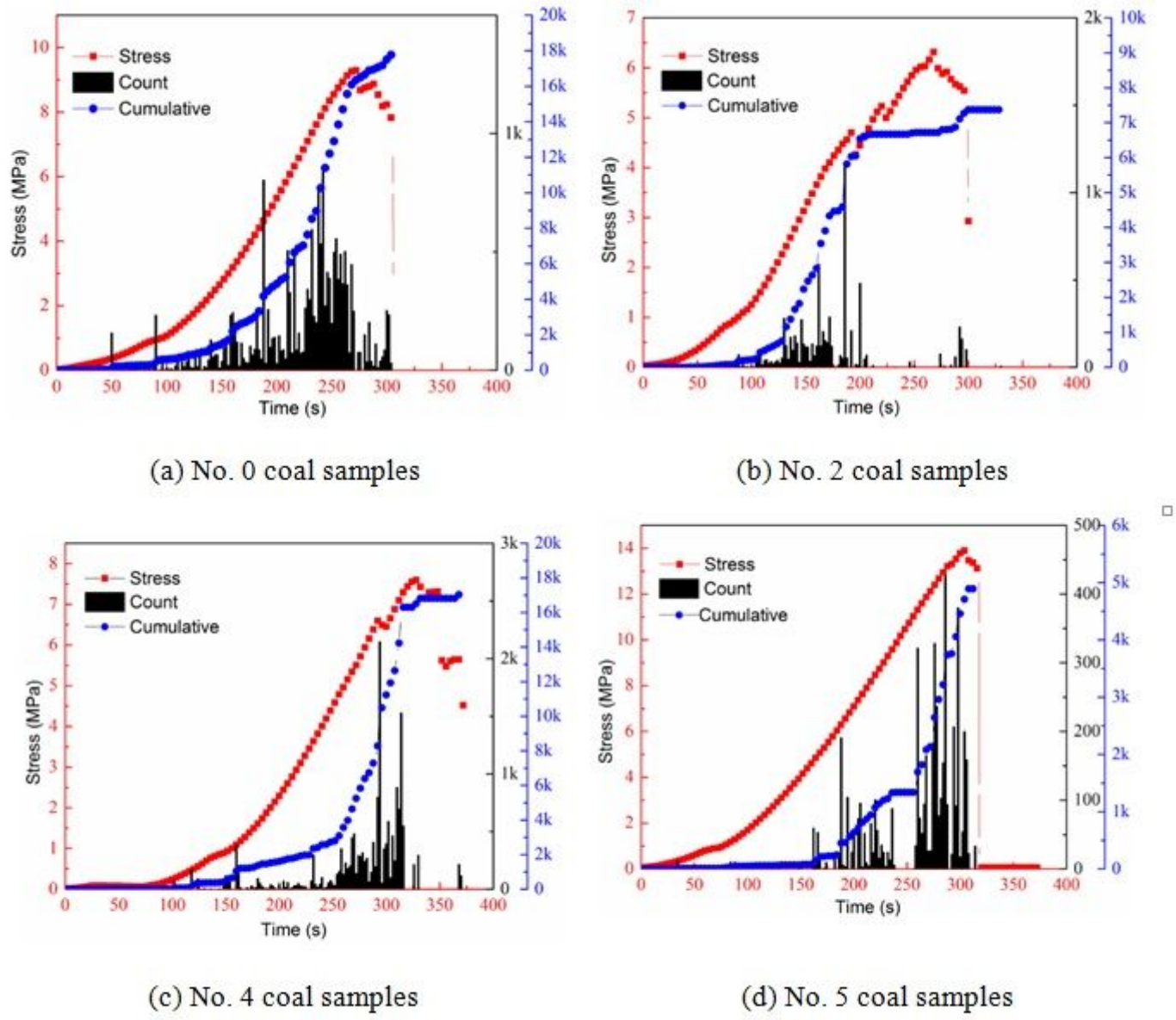

Figure 10

Relationship between AE energy, stress and time

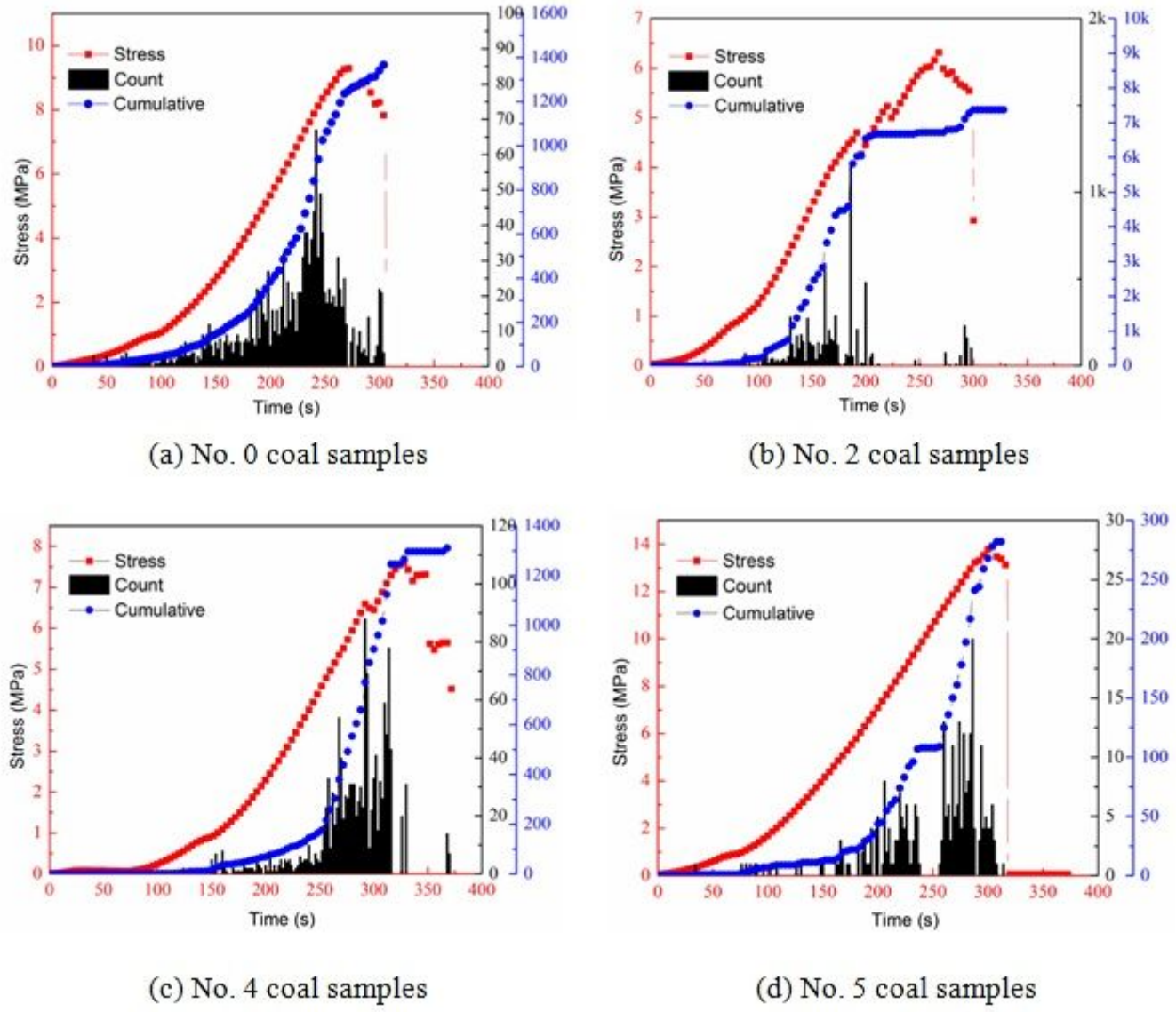

Figure 11

Relationship between AE event, stress and time

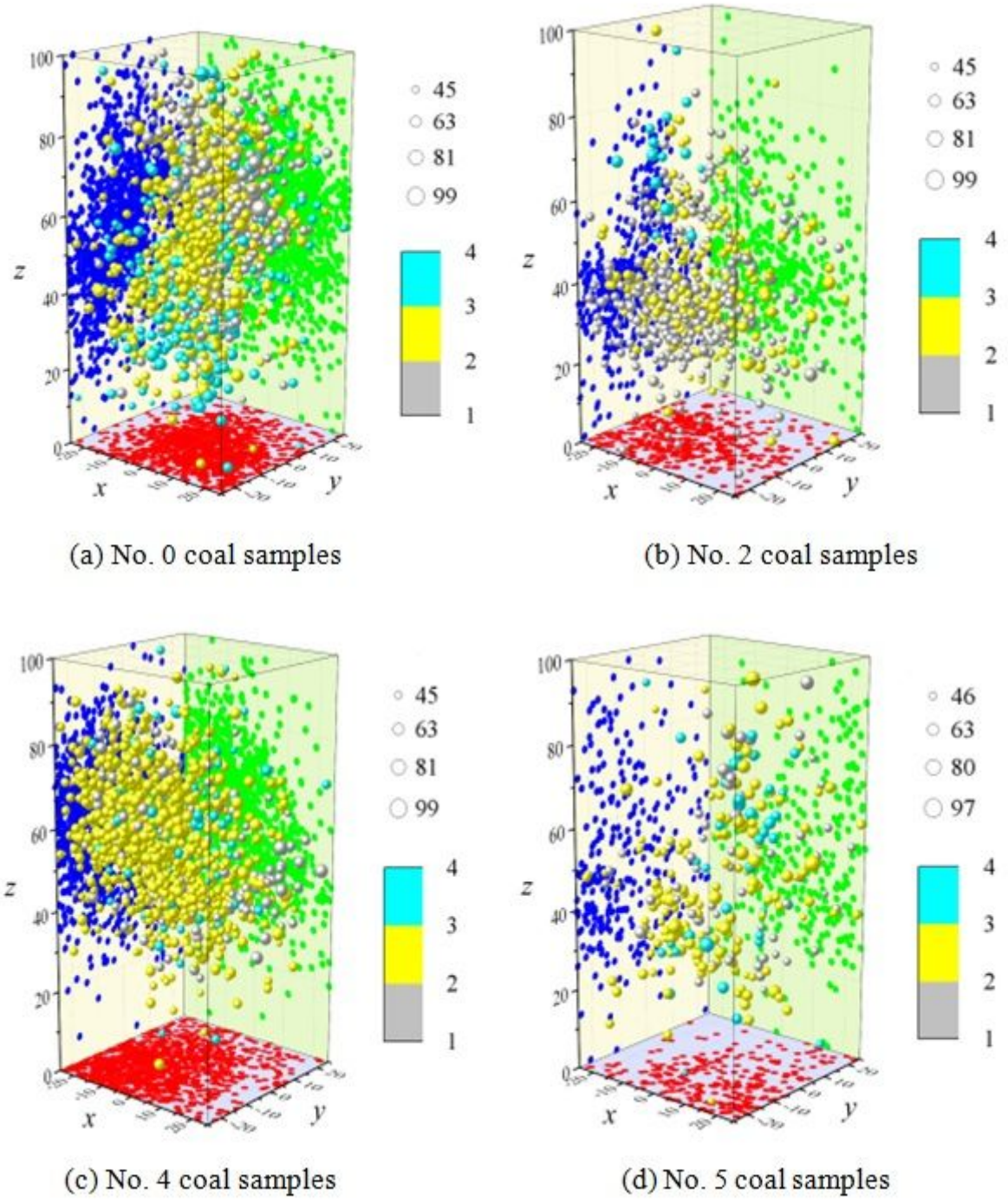

Figure 12

AE source three-dimensional positioning